

# Effect of the Magnetisation of Covered Electrodes on the Quality and Properties of Underwater Wet Welded Joints

---

**Abstract:** The article analyses the effect of the magnetisation of covered electrodes on the geometry and properties of T-joints with fillet welds made of steel S235JR in watery environment. It was established that as regards the conditions and parameters used in the tests, the magnetisation of electrodes affected the stability of arc burning and the formation of shape-related welding imperfections but it did not influence the microstructure and hardness of the test joints.

**Keywords:** underwater welding, wet welding, magnetisation, covered electrode

**DOI:** [10.17729/ebis.2016.3/5](https://doi.org/10.17729/ebis.2016.3/5)

---

## Introduction

Underwater welding is usually used when repairing or modernising structures and their elements, e.g. Jack-Up type foundations of oil rigs, elements reinforcing wharfs, ship platings, pipelines etc. Usually, such elements are made of high strength steels or duplex steels [1-7]. In order to properly perform required repairs, it is necessary to become familiar with phenomena characteristic for a given underwater welding procedure (wet welding, dry welding, welding using local dry chambers) correlated with an implemented welding process [1,2,8-10]. One of the most common welding methods used to a depth of approximately 60 m is wet welding. The characteristic feature of wet welding, regardless of a welding process, is the direct contact of workpieces, welding torches, filler metals and welding fixtures with water [11-13]. Among all underwater welding procedures, wet welding is characterised by the lowest costs (due to

the lack of the necessity of using complicated fixtures) than costs borne when dry welding utilising dedicated chambers [1,8]. During underwater wet welding works, the diver has greater freedom of movement, which significantly affects the efficiency of work. In spite of commonly held opinions, the obtainment of welded joints characterised by good quality and mechanical properties is possible [14]. However, it is necessary to bear in mind the following greatest difficulties accompanying underwater welding [1,2,14-21]:

1. high level of hydrogen diffusing in the weld deposit, as a result of significant amount of steam in the area of arc burning;
2. high cooling rate of welded joints related to the quick discharge of material heat by water. The value of the heat absorption coefficient is higher than in air (even up to a hundred times, depending on the manner of water boiling on the boundary surface of a

---

dr inż. Grzegorz Rogalski (PhD (DSc) Eng.), dr inż. Dariusz Fydrych (PhD (DSc) Eng.);  
mgr inż. Karolina Prokop-Strzelczyńska (MSc Eng.) – Gdańsk University of Technology,  
Institute of Materials Engineering and Joining

- workpiece and a welding position);
- pressure increasing along with an increasing welding depth, unfavourably effecting the behaviour of electric arc, changing phenomena taking place in arc, affecting arc stability and unfavourably influencing the metallurgy of a weld pool;
  - impaired visibility in the welding area caused by welding fumes.

The knowledge of these limitation and the process of specifying a welding procedure in accordance with appropriate standards or regulations (AWS D3.6M: 2010 *Underwater Welding Code; Recommended Practice* DNV-RP-F113 *Pipeline Subsea Repair*; Offshore Standard DNV-OS-F101; EN ISO 15614-9 *Specification and qualification of welding procedures for metallic materials. Welding procedure test. Part 9: Underwater wet welding*) make it possible to determine proper welding parameters and other variables important for the obtainment of adopted criteria. During repairs, one of the most important factors, in addition to diver skills, appropriate power sources or filler metals is proper infrastructure ensuring the safe work of diver-welders and easy access to tools used during underwater works, e.g. pneumatic grinders, brushes supports, covered electrodes etc.

The underwater welding works performed during wharf repair using tight retaining walls (Larsen walls) were accompanied by repeated difficulty maintaining arc stability, which precluded the making of welds or led to the formation of welding imperfections such as irregular weld faces, undercuts and incomplete fusions. The analysis of welding conditions and parameters indicated the magnetisation of covered electrodes as the potential reason for the above named problems. The electrodes were delivered under water (to the place of the welding works) using a permanent magnet, magnetising the electrodes. The overview of reference publications did not make it possible to verify the above mentioned hypothesis, therefore it was necessary to schedule and perform appropriate

tests aimed to determine how the magnetisation of covered electrodes used during underwater wet welding (process 111) affected the structure and properties of welded joints.

## Materials, Welding Conditions and Testing Methods

The tests involved the use of an 8.00 mm thick sheet made of non-alloy structural steel S235JR (1.0038). The chemical composition and mechanical properties of the steel are presented in Tables 1 and 2. The tests were performed using the following schedule:

- Development of an appropriate welding procedure specification (WPS) on the basis of a related record of welding parameters.
- Wet welding of two-sided test T-joints with fillet welds, performed using magnetised electrodes (one side of the joints) and non-magnetised electrodes (the other side of the joints).
- Making test joints in accordance with related standards:
  - visual tests (VT),
  - magnetic particle tests (MT),
  - macro and microscopic metallographic tests,
  - Vickers hardness tests (HV10).

The test joints were made in accordance with a related welding procedure specification (WPS) in an open freshwater basin at a depth of 8.0 m. Welding was performed using electrodes having a higher content of Ni, intended for the underwater joining of non-alloy structural steels. The Barracuda Gold electrodes designated according to EN ISO 2560-A as E 46 2 1Ni RR 51 had a diameter of 4.0 mm. The chemical composition and mechanical properties of the weld deposit are presented in Tables 3 and 4. The temperature of water in the welding area amounted to 9°C. Joints were made in a horizontal position (PB) using direct current with negative polarity. The electrodes were magnetised by a permanent magnet while being lowered under water (for a typical time of approximately 1 min). In order

to eliminate an accidental result, it was necessary to make two test joints in similar conditions, in accordance with the parameters presented in Table 5. The specimens were designated with the following symbols: w01, w02 - specimen numbers, NM – a specimen made using a non-magnetised electrode, M – a specimen made using a magnetised electrode and a number. Figures 1

and 2 present the test joints.

## Test Results

### Non-Destructive Tests

The visual tests (VT) and magnetic particle tests (MT) were performed in accordance with related standards, i.e. PN-EN ISO 17637:2011 and

Table 1. Chemical composition of steel S235JR

Contents of chemical elements, % by weight *					
C	Mn	Si	P	S	N
0.17	1.4	-	0.035	0.035	0.012

\* Chemical composition according to standard PN-EN 10025-2 (Hot-rolled products of structural steels. Part 2: Technical delivery conditions for non-alloy structural steels)

Table 2. Mechanical properties of steel S235JR

T [°C]	Re <sub>H</sub> [MPa]	Rm [MPa]	A <sub>5</sub> [%]	KV [J]
20	235	360÷510	20	27 (-20÷20°C)

\* Mechanical properties according to standard PN-EN 10025-2 (Hot-rolled products of structural steels. Part 2: Technical delivery conditions for non-alloy structural steels)

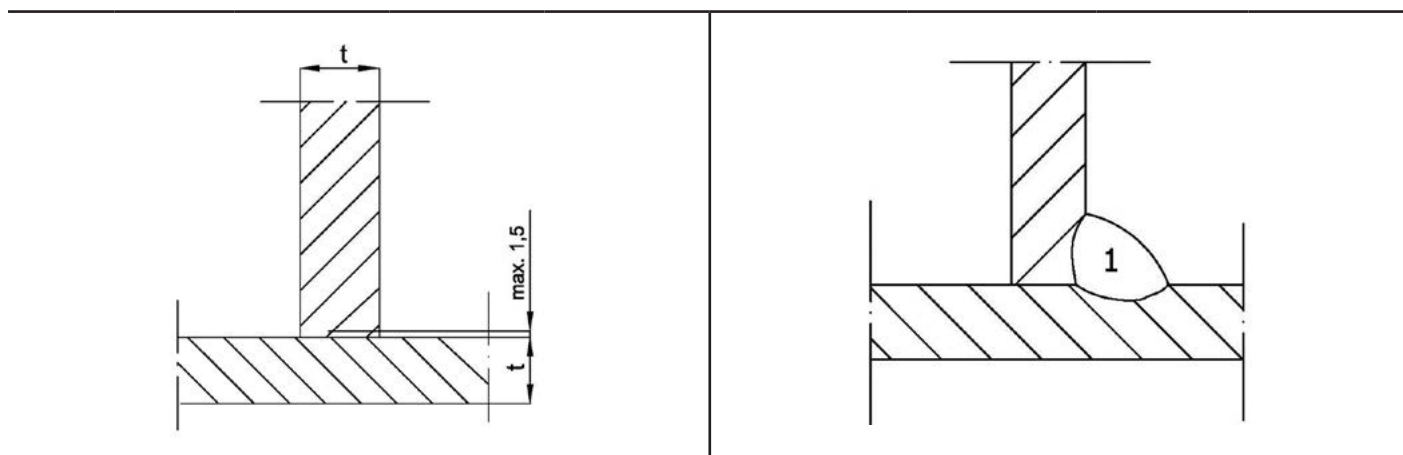
Table 3. Chemical composition of the weld deposit of Barracuda Gold covered electrodes [22]

Contents of chemical elements, % by weight *					
C	Mn	S	Si	P	Ni
0.05	0.5	0.45	0.025	0.025	0.3

Table 4. Mechanical properties of the weld deposit of Barracuda Gold covered electrodes [22]

	Re <sub>H</sub> [MPa]	A <sub>5</sub> [%]	KV [J]
Air	540	26	62 [0°C]
Water	564	12÷13,5	50÷54 [-20°C]

Table 5. Geometry and welding parameters used when making the test joints



Run	Process	Filler metal size [mm]	Current [A]	Arc voltage [V]	Current type/polarity	Filler metal wire feeding rate [m/min]	Welding rate [mm/s]	Heat input [kJ/mm]
1	111	4.0	190÷200	25÷26	DC/-	-	3.4	0.59÷1.22



PN-EN ISO 9934-1:2015. During welding performed using the magnetised electrodes, arc was burning in an unstable manner. As a result, the process was accompanied by difficulties maintaining arc and had to be stopped. Because of the above named problems, it was not possible to use the entire electrode when making a welded joint. The specimens were characterised by the improper geometry of the welds made using the magnetised electrodes. The welds were characterised by improper faces, areas of increased excess weld metal and spatters. A small fragment of the specimen also contained incomplete fusions (Fig. 3). The welds made using the non-magnetised electrodes were free from the above named imperfections. None of the specimens contained cracks or porosity.

### Macro and Microscopic Metallographic Tests

The macro and microscopic metallographic tests were performed in accordance with the guidelines of standard PN-EN ISO 17639. The specimens were cut out of the central part of the joints, transversely in relation to the weld axis. The specimen surfaces were prepared by grinding and polishing, and etching using Nital reagent. Figure 4 presents the macrostructure of the test joints.

The results of the macroscopic tests confirmed the results of the non-destructive tests. Both sides of the specimen contained small undercuts, which due to their geometry enabled the classification of the specimen as representing quality level B according to PN-EN ISO 5817:2014. The welds on the right side of the joints (made using the magnetised electrodes) were characterised by excess weld face penetration with a characteristic change in the cross-section, probably caused by the effect of the disturbed electromagnetic field during welding. This phenomenon was present along the entire length of the welded joints. The joints were free from welding imperfections. The edges of the elements were properly melted. The

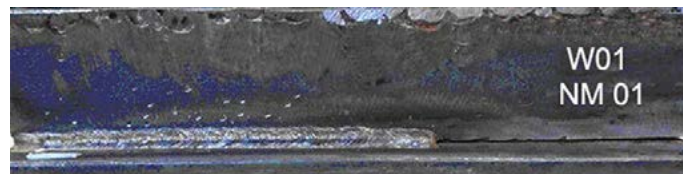


Fig. 1. T-joint with the fillet weld (FW) on the side welded using a non-magnetised electrode

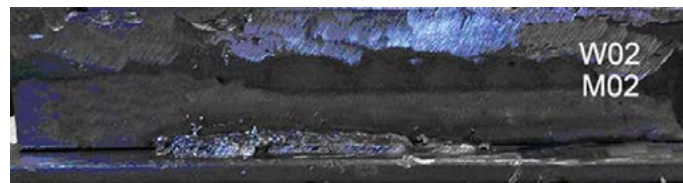


Fig. 2. T-joint with the fillet weld (FW) on the side welded using a magnetised electrode

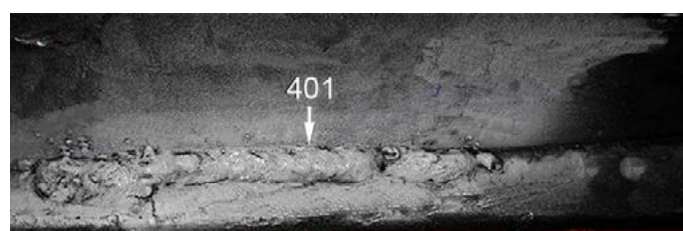


Fig. 3. T-joint with the fillet weld (FW) on the side welded using a magnetised electrode, after magnetic particle tests; visible welding imperfections: spatters, the irregularly shaped weld face and incomplete fusion (designated with the arrow)

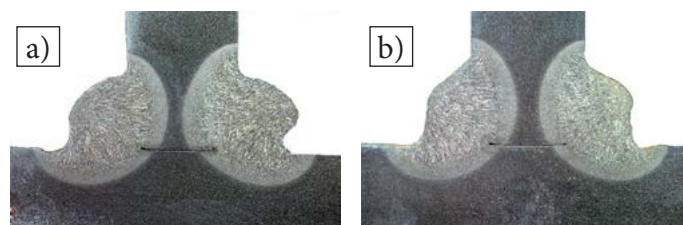


Fig. 4. Cross-section of the test joints: a) specimen W01 – left: weld NM01, right: weld M01; b) specimen W02 – left: weld NM02, right: weld M02; free from welding imperfections; etchant: Nital

HAZ was regular on both sides of the joints, which could imply the uniform distribution of heat in the entire specimen.

The microscopic metallographic tests involved the use of the specimens previously used in the macroscopic tests. The specimens were subjected to further processing stages and prepared for etching using Nital. Figures 5-9 present the structure of welded joint areas. The structure of the base material was characteristic of steel S235JR, i.e. ferritic-pearlitic with clearly visible grain boundaries (Fig. 5).



The weld structure contained ferrite and pearlite grains arranged in a columnar manner in the direction of metal solidification (Fig. 6). The HAZ area was characterised by slight grain growth. The area of superheating did not contain hardening structures (martensite and bainite).

The microscopic observations did not reveal significant differences in the structures of the

joints made with magnetised electrodes and those made using non-magnetised electrodes. The tested areas did not contain welding micro-imperfections i.e. microcracks, slag inclusions, incomplete microfusions, which were expected particularly in terms of welding performed using magnetised electrodes. The observed structures demonstrated the proper adjustment of welding parameters.

### Hardness Measurements of the Welded Joints

The hardness measurements were performed in accordance with the requirements of standard PN-EN ISO 9015-1:2011 *Welding. Destructive tests on welds in metallic materials. Hardness test on arc welded joints*. The tests were performed using a VEB hardness tester. The indenter load amounted to 98 N (HV10). On the basis of Offshore Standard DNV-OS-C401 (Fabrication and Testing of Offshore Structures April 2013, the

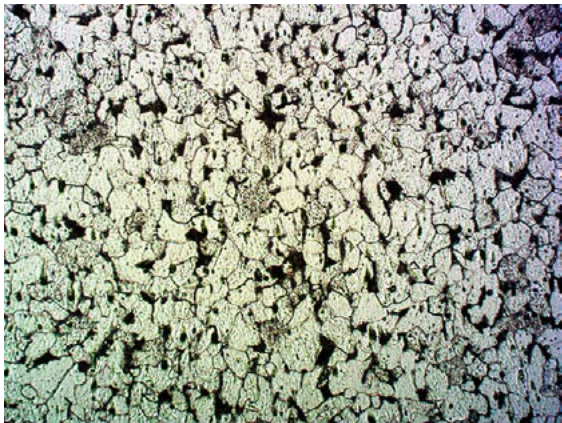


Fig. 5. Microstructure of steel S235JR; etchant: Nital; mag. 200x

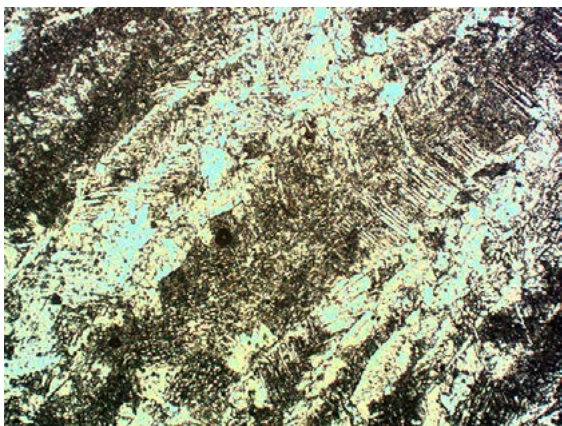


Fig. 6. Microstructure of the weld in joint NM01; etchant: Nital; mag. 200x

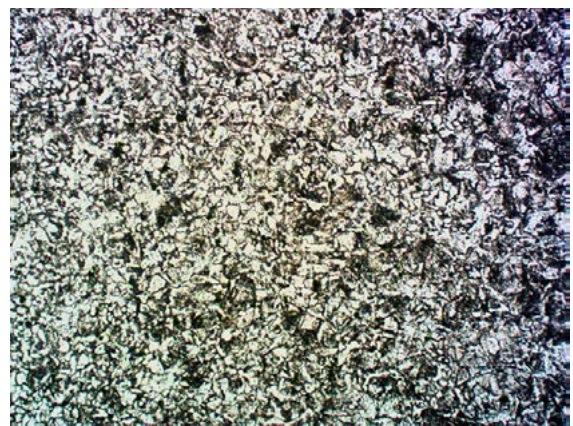


Fig. 8. Microstructure of the HAZ in joint NM01; etchant: Nital; mag. 200x



Fig. 7. Microstructure of the weld in joint M01; etchant: Nital; mag. 200x



Fig. 9. Microstructure of the HAZ in joint M01; etchant: Nital; mag. 200x



acceptance criterion adopted for the steel grade used in the tests (material group 1.1 according to TR ISO 15608) was at a level of 350 HV<sub>10</sub>. The Vickers hardness test was performed along a line located 2 mm away from the weld face and sheet surface (Fig. 10). The cross-sectional hardness distribution related to the test joints is presented in Figures 11 and 12. The hardness distribution is typical of joints welded with a filler metal characterised by greater strength than the strength of the base material. The analysis of the minimum (Fig. 12: 125 HV<sub>10</sub>) and the maximum (Fig. 11: 330 HV<sub>10</sub>) HAZ hardness-related individual values justified the assumption that they represented gross errors not subjected to interpretation. The analysis of hardness-related results revealed that the magnetisation of electrodes did not significantly affect the hardness of the joints. For the welding parameters used in the tests (Table V), the obtained results were below the adopted acceptance criterion (350 HV<sub>10</sub>).

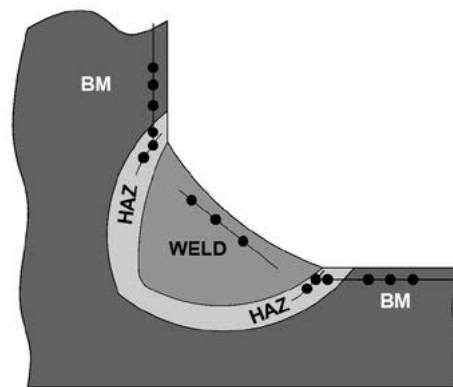


Fig. 10. Arrangement of the measurement points on the cross-section of the welded joint

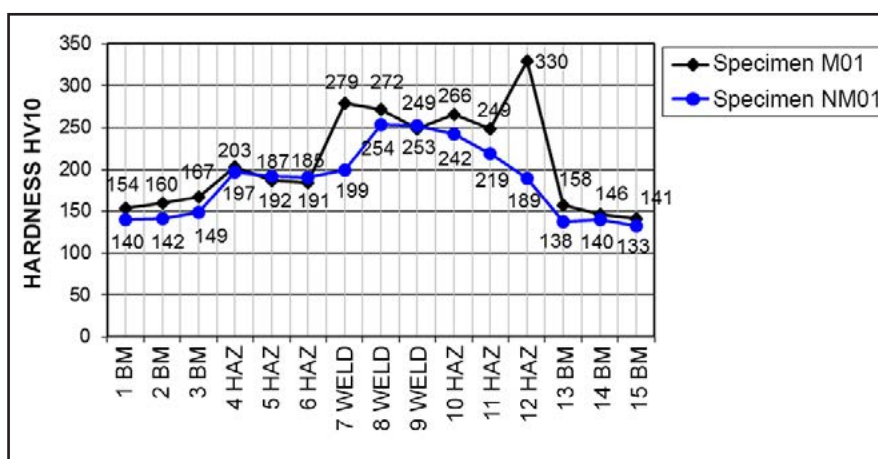


Fig. 11. Hardness distribution in joint W01: NM01 and M01

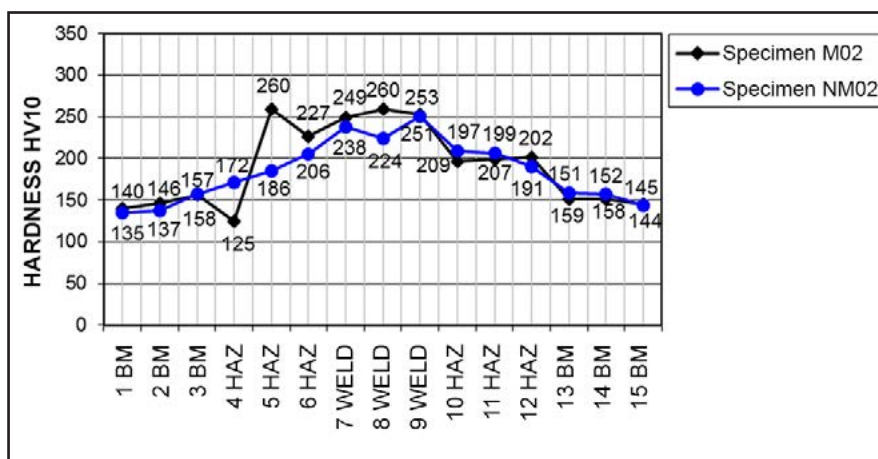


Fig. 12. Hardness distribution in joint W02: NM02 and M02

### Summary

The work is concerned with the assessment of the effect of the magnetisation of covered electrodes on the quality of underwater wet welded joints. The tests involved making joints in natural conditions, using magnetised electrodes and electrodes in the as-delivered state. The visual tests (VT) and magnetic particle tests (MT) of the joints revealed the disturbed geometry of the welds made using the magnetised electrodes, i.e. excess weld face penetration with a characteristic change in the cross-section, probably caused by the disturbance of the electromagnetic field affecting the stability of arc burning. Arc burning in an unstable manner could also lead to the formation of incomplete fusions, undercuts

and spatters. The macroscopic tests did not reveal the presence of cracks, inclusions and other discontinuities. The microscopic tests did not reveal differences in the structure of both variants of test joints. The magnetisation of covered electrodes did not significantly affect the values and shape of hardness distribution. The values obtained were below the adopted acceptance criterion of 350 HV<sub>10</sub>, which demonstrated

the good weldability of the tested steel in experimental conditions.

It should be noted that thermal processes, which during underwater welding are decisive for the creation of brittle structures, are also significantly affected by the shape of a joint. The research involved the testing of T-joints, the geometry of which restricts mechanisms of heat discharge from the material (bubble and membrane boiling processes, convection, radiation and conduction between media). The presented conclusions should be verified by testing the phenomenon described above in relation to other important variables (other steel grades and shapes of joints).

## Conclusions

During the underwater wet welding performed using covered electrodes and adopted welding conditions and parameters, the magnetisation of electrodes affected the stability of arc burning and the formation of shape-related welding imperfections, yet it did not influence the microstructure and hardness of the test T-joints.

## References

- [1] Rowe M., Liu S.: *Recent developments in underwater wet welding*. Science and Technology of Welding and Joining, 2001, no. 6, pp. 387-396  
<http://dx.doi.org/10.1179/stw.2001.6.6.387>
- [2] Fydrych D., Rogalski G., Łabanowski J.: *Problems of underwater welding of higher-strength low alloy steels*. Biuletyn Instytutu Spawalnictwa, 2014, no. 5, pp. 187-195  
[http://bulletin.is.gliwice.pl/index.php?go=current&ebis=2014\\_05\\_25](http://bulletin.is.gliwice.pl/index.php?go=current&ebis=2014_05_25)
- [3] Sun Q.J., Cheng W.Q., Liu Y.B., Wang J.F., Cai C.W., Feng J.C.: *Microstructure and mechanical properties of ultrasonic assisted underwater wet welding joints*. Materials & Design, 2016, vol. 103, pp. 63-70  
<http://dx.doi.org/10.1016/j.matdes.2016.04.019>
- [4] Skorupa A., Bal M.: *Wpływ środowiska wodnego na jakość połączeń spawanych pod wodą*. Przegląd Spawalnictwa, 1986, no. 3.
- [5] Skorupa A., Masłowski A., Bal M.: *Wytrzymałość połączeń spawanych pod wodą metodą hiperbaryczną*. Przegląd Spawalnictwa, 1996, no. 3.
- [6] Rodriguez-Sanchez J.E., Perez-Guerrero F., Liu S., Rodriguez-Castellanos A., Albiter-Hernandez A.: *Underwater repair of fatigue cracks by gas tungsten arc welding process*. Fatigue & Fracture of Engineering Materials & Structures, 2014, no. 6.  
<http://dx.doi.org/10.1111/ffe.12146>
- [7] Rogalski G., Fydrych D., Łabanowski J.: *Oceana możliwości naprawy rurociągu podwodnego ze stali API 5L X65 przy zastosowaniu spawania mokrego*. Przegląd Spawalnictwa, 2015, no. 5.
- [8] Xue L., Wu J., Huang J., Huang J., Zou Y., Liu J.: *Welding polarity effects on weld spatters and bead geometry of hyperbaric dry GMAW*. Chinese Journal of Mechanical Engineering, 2016, vol. 29, issue 2, pp 351-356  
<http://dx.doi.org/10.3901/cjme.2015.1104.131>
- [9] Rogalski G., Łabanowski J., Fydrych D., Tomków J.: *Bead-on-plate welding on S235JR steel by underwater local dry chamber process*. Polish Maritime Research, 2014, no. 2, pp. 58-64  
<http://dx.doi.org/10.2478/pomr-2014-0020>
- [10] Rogalski G., Fydrych D., Łabanowski J.: *Oceana możliwości spawania pod wodą drutem prozkowym metodą lokalnej komory suchej*. Biuletyn Instytutu Spawalnictwa, 2012, no. 5.
- [11] Fydrych D., Rogalski G., Świerczyńska A., Łabanowski J.: *Ocena przydatności komercyjnych elektrod otulonych do spawania mokrego pod wodą z wykorzystaniem analizy skupień*. Przegląd Spawalnictwa, 2015, no. 10.
- [12] Rogalski G., Łabanowski J.: *Certyfikowanie nurków-spawaczy przy spawaniu mokrym pod wodą w warunkach hiperbarycznych*. Biuletyn Instytutu Spawalnictwa, 2011, no. 1.
- [13] Rogalski G.: *Wpływ niezgodności spawalniczych na właściwości mechaniczne złączy*

- spawanych pod wodą metodą mokrą. Przegląd Spawalnictwa, 2012, no. 12.
- [14] Santos V.R., Monteiro M.J., Rizzo F.C., Bracarense A.Q., Pessoa E.C.P., Marinho R.R., Vieira L.A.: *Development of an oxy-rutile electrode for wet welding*. Welding Journal, 2012, no. 12.
- [15] Guo N., Guo W., Xu C., Du Y., Feng J.: *Effect of boric acid concentration on viscosity of slag and property of weld metal obtained from underwater wet welding*. Journal of Materials Engineering and Performance, 2015, no. 6, pp. 2563–2568  
<http://dx.doi.org/10.1007/s11665-015-1528-8>
- [16] Guo N., Yang Z., Wang M., Yuan X., Feng J.: *Microstructure and mechanical properties of an underwater wet welded dissimilar ferritic/austenitic steel joint*. Strength of Materials, 2015, no. 1, pp. 12–18  
<http://dx.doi.org/10.1007/s11223-015-9622-6>
- [17] Guo N., Wang M., Du Y., Guo W., Feng J.: *Metal transfer in underwater flux-cored wire wet welding at shallow water depth*. Materials Letters, 2015, vol. 144, pp. 90–92  
<http://dx.doi.org/10.1016/j.matlet.2015.01.033>
- [18] Guo N., Xu C., Guo W., Du Y., Feng J.: *Characterization of spatter in underwater wet welding by X-ray transmission method*. Materials & Design, 2015, vol. 85, pp. 156–161.  
<http://dx.doi.org/10.1016/j.matdes.2015.06.152>
- [19] Fydrych D., Świerczyńska A., Rogalski G.: *Effect of underwater wet welding conditions on the diffusible hydrogen content in deposited metal*. Solid State Phenomena, 2012, vol. 183, pp. 193–200.  
<http://dx.doi.org/10.4028/www.scientific.net/ssp.183.193>
- [20] Fydrych D., Łabanowski J., Rogalski G., Haras J., Tomków J., Świerczyńska A., Jakóbczak P., Kostro Ł.: *Weldability of S500MC steel in underwater conditions*. Advances in Materials Science, 2014, no. 2.  
<http://dx.doi.org/10.2478/adms-2014-0008>
- [21] Fydrych D., Łabanowski J., Tomków J., Rogalski G.: *Cold cracking of underwater wet welded S355G10+ N high strength steel*. Advances in Materials Science, 2015, no. 3.  
<http://dx.doi.org/10.1515/adms-2015-0015>
- [22] <http://www.specialwelds.com>